Short communication

Improved anticorrosion properties and electrical conductivity of 316L stainless steel as bipolar plate for proton exchange membrane fuel cell by lower temperature chromizing treatment

Lijun Yang, Haijun Yu *, Lijun Jiang, Lei Zhu, Xuyu Jian, Zhong Wang

Energy Materials and Technology Research Institute, Beijing General Research Institute for Nonferrous Metals, Beijing 100088, China

ABSTRACT

The lower temperature chromizing treatment is developed to modify 316L stainless steel (SS 316L) for the application of bipolar plate in proton exchange membrane fuel cell (PEMFC). The treatment is performed to produce a coating, containing mainly Cr-carbide and Cr-nitride, on the substrate to improve the anticorrosion properties and electrical conductivity between the bipolar plate and carbon paper. Shot peening is used as the pretreatment to produce an activated surface on stainless steel to reduce chromizing temperature. Anticorrosion properties and interfacial contact resistance (ICR) are investigated in this study. Results show that the chromized SS 316L exhibits better corrosion resistance and lower ICR value than those of bare SS 316L. The chromized SS 316L shows the passive current density about $3E−7\,A\,cm^{-2}$ that is about four orders of magnitude lower than that of bare SS 316L. ICR value of the chromized SS 316L is $13\,m\Omega\,cm^2$ that is about one-third of bare SS 316L at $200\,N\,cm^{-2}$ compaction forces. Therefore, this study clearly states the performance advantages of using chromized SS 316L by lower temperature chromizing treatment as bipolar plate for PEMFC.

1. Introduction

The proton exchange membrane fuel cell (PEMFC) is an ideal candidate for automotive propulsion application due to its high efficiency and cleanliness [1,2]. Bipolar plate is a major part of PEMFC stack, which accounts for most of the total weight and cost of stacks [3]. Currently, machined graphite composites are mainly used for bipolar plate for PEMFC, however, their high cost of machining limit their wide application. Much effort has focused on metal bipolar plates [4] because of their malleable and superior mechanical properties. Among many candidate materials for metal bipolar plates, stainless steel has attracted much attention due to its mechanical properties and relatively low price [5,6]. Nevertheless, stainless steel is apt to be corroded in PEMFC working environment. Therefore, coating a protective film with good corrosion resistance and electrical conductivity is considered to be one of the effective solutions to overcome the shortcomings of stainless steel. A number of coating techniques including chemical vapor deposition (CVD) [7], physical vapor deposition (PVD) [8], electro-plating [9], and chromizing [10] have been investigated to apply to modify the metal bipolar plate of PEMFC. Chromizing is considered to be an effective surface treatment to improve corrosion resistance of bipolar plate since it produces a uniform diffuse layer on the surface and maintains high coherence at the interface between the diffuse layer and the substrate [10–12]. However, nearly all conventional chromizing processes are carried out at temperature above $1000\,°C$ that will induce serious distortion of work pieces and severe degradation of mechanical properties [13,14]. Void formation has also been reported after the pack cementation of Cr due to Kirkendall effect [7]. To minimize these negative effects, it is necessary to reduce chromizing temperature. Wang et al. [15] have investigated a duplex lower temperature chromizing process on low carbon steel after surface mechanical attrition treatment, and results show that corrosion resistance was improved markedly.

In this study, a novel lower temperature chromizing process was developed. It is a simpler process compared with Wang's method. The pretreatment of shot peening was utilized before chromizing since it would induce numerous grain boundaries to enhance atomic diffusion and chemical reaction kinetics [16–18]. Then a lower temperature chromizing treatment followed to form a Cr-enriched film on SS 316L. Microstructure, interfacial contact resistance (ICR) and corrosion resistance of chromized SS 316L were investigated.

* Corresponding author. Tel.: +86 10 8224 1239; fax: +86 10 8224 1239.
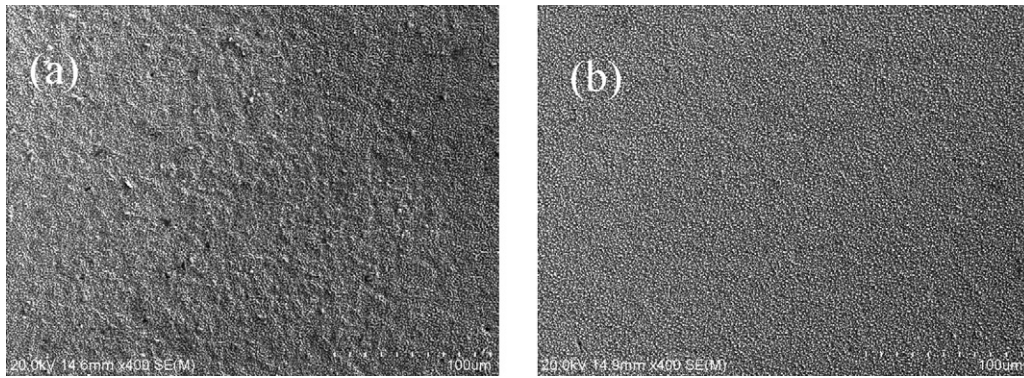*E-mail address:* yuhaijunneu@163.com (H. Yu).

Fig. 1. SEM micrographs of (a) sample A and (b) sample B.

2. Experiments

2.1. Samples preparation

SS 316L sheets (4 mm thick) were chosen as the base metal of bipolar plate. The chemical composition of SS 316L sheets used in this study is listed in Table 1. The sheets were cut into samples of 10 mm × 10 mm, polished with 120, 600, 800 grit SiC abrasive paper, and then carried out by shot peening pretreatment for 10 min. The pack powder mixture used as chromizing deposition source contained a master metal Cr (50 wt.%), inter-filler Al_2O_3 (43 wt.%) and an activator NH_4Cl (7 wt.%). The power mixture was mixed up in accordance with a suitable proportion and homogenized using ball mill for 10 h. The sample was buried in pack powder and chromized for 180 min at 900 °C in Ar atmosphere. In order to compare with the lower temperature chromizing treatment, conventional chromizing treatment was also investigated in this study. In conventional chromizing process, the sample was directly buried in pack powder without carrying out pretreatment and chromized for 180 min at 1100 °C in Ar atmosphere. In this study, process 1 represents the lower temperature chromizing process and process 2 represents the conventional chromizing process.

2.2. Microstructure characterization

The phrase identification of surface of chromized SS 316L was identified by X-ray diffraction (XRD) using an X-Pert Pro with Cu Kα radiation (λ = 1.54178 Å). The morphology of chromized SS 316L was observed by using a scanning electron microscope (SEM, Hitachi S-4800). Meanwhile, the chemical composition of chromized layers and distributions of the Cr and Fe in the chromized layers were monitored by X-ray energy dispersion spectrometer (EDS).

2.3. Electrochemical tests

Both potentiodynamic tests and potentiostatic tests were performed to analyze corrosion characteristics of bare SS 316L and chromized SS 316L. A conventional three-electrode system was used with a working electrode, a platinum sheet as the counter electrode and a standard calomel electrode (SCE) as the reference electrode. Princeton Applied Research 2273 was utilized to conduct these electrochemical experiments. Potentiodynamic tests were

Table 2
Surface chemical composition (wt.%) of chromized SS 316L.

Specimens	Cr	Fe	C	N
Sample A	80.69	5.15	6.22	7.94
Sample B	82.44	6.66	9.39	1.51

conducted in 0.5 M H_2SO_4 + 2 ppm F$^-$ solution at room temperature at the sweeping potential ranged from −0.35 V to 1.0 V (versus SCE) with a scanning rate of 1 mV s^{-1}. To simulate aggressive PEMFC working environment, potentiostatic tests were chosen: at anode, the applied potential was −0.1 V (versus SCE) and solution was purged with hydrogen gas for a simulated PEMFC anode environment, at cathode, the applied potential was 0.6 V (versus SCE) and purged with air for a simulated PEMFC cathode environment, all potentiostatic tests were conducted at 70 °C [19,20].

2.4. ICR measurement

The measurements of ICR between chromized stainless steel and carbon paper were performed using Wang's methods [6,21]. Two pieces of treated conductive carbon paper were sandwiched between the samples and two copper plates. A current of 1 A was applied via two copper plates and voltage drop was measured. And ICR was obtained from the voltage drop.

3. Results and discussion

3.1. Microstructure of the chromized SS 316L

Surface SEM micrographs of chromized SS 316L, shown in Fig. 1(a) and (b), indicate that a flat and continuous chromized layer was deposited on SS 316L. Fig. 1(a) and (b) are surface morphology of sample A (using process 1) and sample B (using process 2), respectively. Surface morphology of sample A is a little coarser than that of sample B, which should be due to the 10 min's shot peening pretreatment. The chemical composition of chromized layers evaluated from the EDS data is shown in Table 2. Results indicate that various carbides and nitrides of chromium are formed in the surface of chromized SS 316L. The formation of chromium carbides result from the diffusions of Cr inwards and carbon outwards [18,22], because of the larger Gibbs free energy changes for the formation of chromium carbides than that of the cementite. And nitrides nucleate and grow inward from the top surface,

Table 1
Chemical composition (wt.%) of SS 316L.

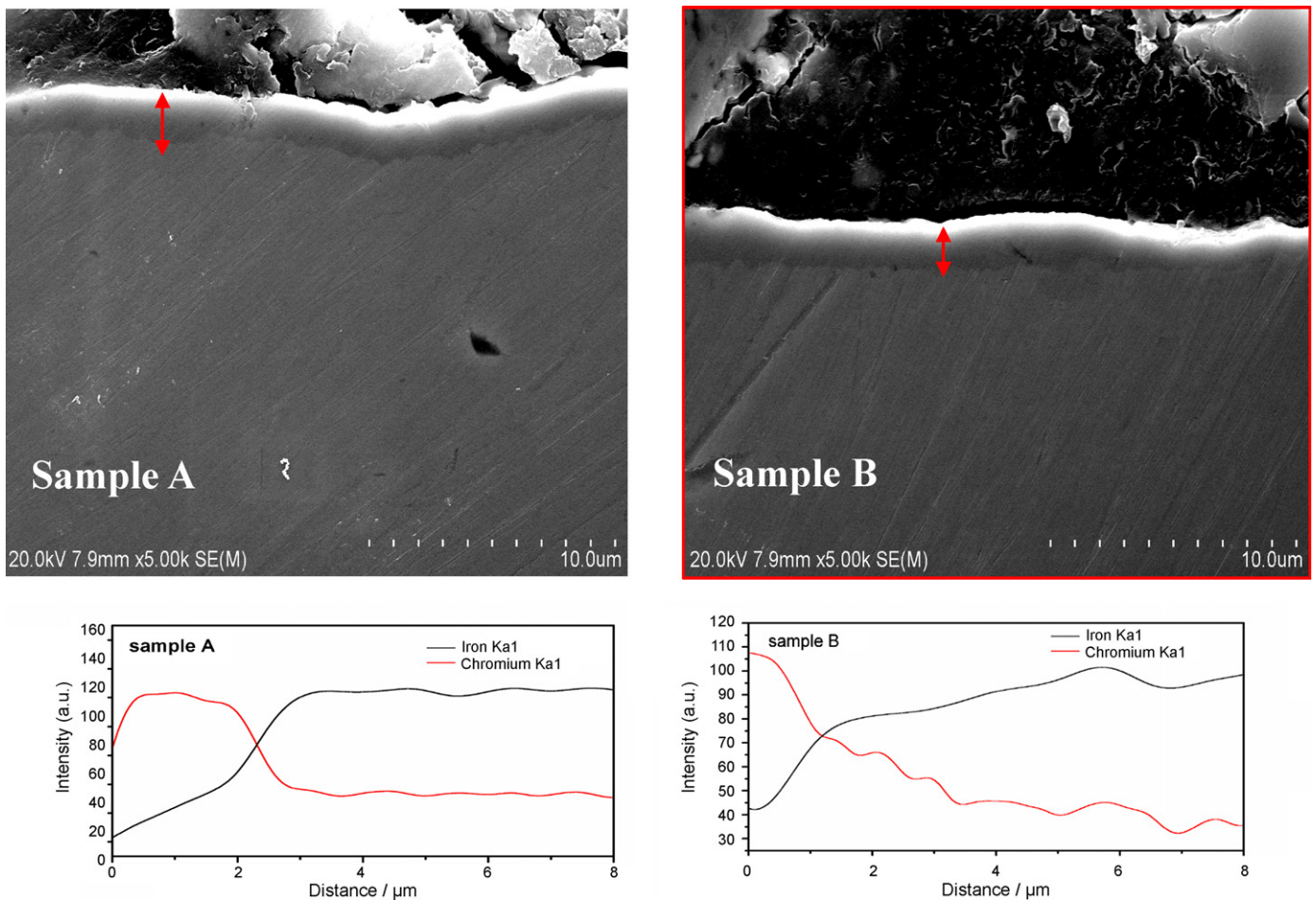| Materials	C	Mn	Si	S	P	Cr	Ni	Cu	Mo	N
316L	0.022	1.49	0.34	0.01	0.028	16.45	10.81	0.45	2.04	0.03

Fig. 2. Cross-sectional SEM micrograph of samples A and B, and followed by concentration profile of Fe and Cr across Cr-rich layer after chromizing process 1 and 2.

with the reactions of diffused chromium and nitrogen atoms [23]. Fig. 2 is cross-sectional SEM micrographs with elemental line scan of chromized SS 316L. It is clear that an obvious and continuous chromized layer is deposited on the substrate. Cr-enriched layer about 2 μm is formed in sample A, which is thicker than that of sample B (about 1 μm). The thicker chromized layer is due to faster diffusion kinetics of the deposited Cr in the layer of sample A.

XRD patterns (Fig. 3) show that various Cr-rich phrases, mainly $Cr_{23}C_6$ and Cr_2N phrase, are formed in the surface layers. Combing with the surface chemical composition analysis by EDS, it can be estimated that a continuous Cr-enriched diffusion layer, containing major Cr-carbides and Cr-nitrides, is formed on SS 316L. And a larger volume fraction of nitride in sample A than that in sample B could also be indicated.

Formation of a thicker chromized surface layer, with a lower chromizing temperature, is obtained by the enhanced diffusivity and phase formation kinetics [18]. A large volume of grain boundaries with a high excess stored energy introduced by the pretreatment of shot peening can promote the diffusion and deposition rate of Cr in the surface layer. Hence, we can obtain a thicker and dense Cr-enriched surface layer at a relative lower temperature.

3.2. Corrosion resistance

Potentiodynamic tests were carried out to investigate polarization behavior of chromized SS 316L in 0.5 M H_2SO_4 + 2 ppm F^- solution at room temperature. Fig. 4 is polarization curves for bare SS 316L and chromized SS 316L (both samples A and B). It is noted that chromized SS 316L was in passive state under test condi-

tion with passive current densities about $3E-7\,A\,cm^{-2}$, which were about four orders of magnitude lower than that of bare SS 316L. It indicates the effectiveness of chromium compounds on the surface layer in improving anticorrosion properties of stainless steel. The
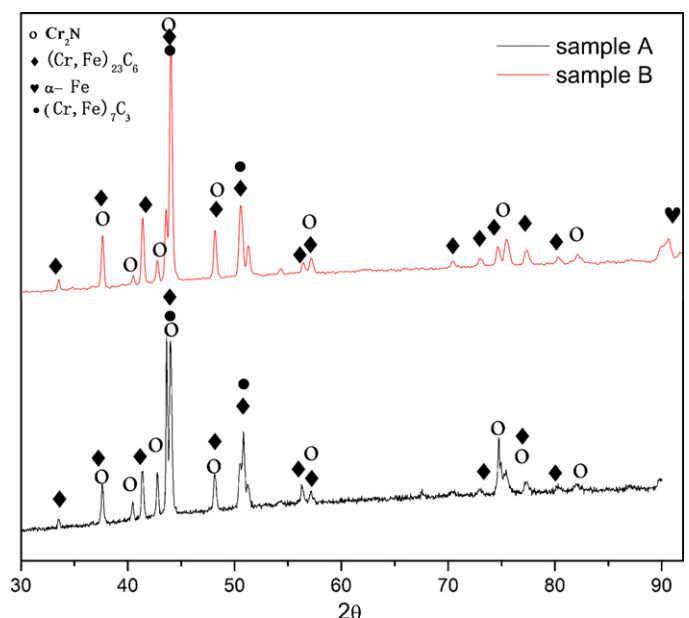

Fig. 3. XRD patterns of samples A and B after chromizing process 1 and 2.
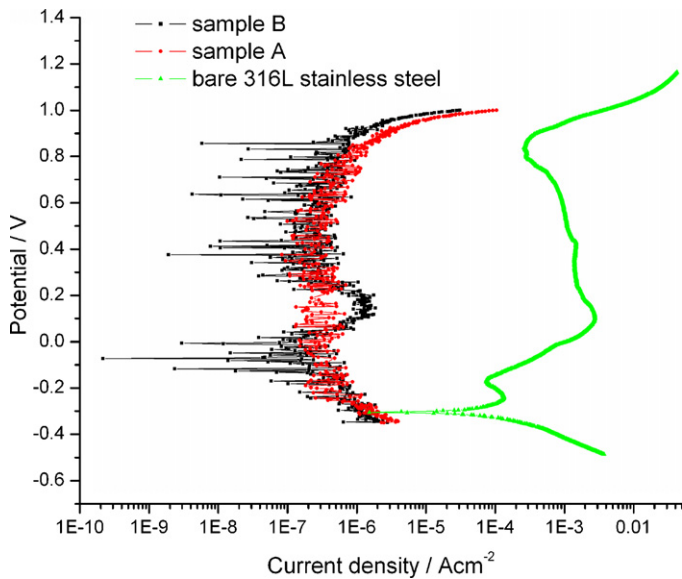
Fig. 4. Potentiodynamic polarization curves obtained from bare SS 316L, samples A and B.

Cr-enriched layers make chromized SS 316L in passive state under simulated PEMFC working condition and therefore protect SS 316L against further corrosion.

To compare the long-term corrosion resistance of chromized SS 316L, potentiostatic tests were conducted under simulated PEMFC working condition by applying −0.1 V to anode and 0.6 V to cathode. The anode was purged with hydrogen gas and cathode was purged with air in 0.5 M H_2SO_4 + 2 ppm F^- solution at 70 °C. Potentiostatic curves of samples A and B measured at simulated anode and cathode working condition are shown in Fig. 5(a) and (b). From Fig. 5(a), it can be seen that chromized SS 316L exhibits low and stable current densities for an extended period of time that demonstrate the effectiveness of chromizing processes in improving the corrosion resistance of stainless steel. The current density of sample A (about 7.5E−8 A cm^{-2}) is about one order of magnitude lower than that of sample B (about 3.5E−7 A cm^{-2}). These negative current densities due to the hydrogen gas purged in the solution providing a reductive environment and then provide cathodic protection for chromized SS 316L. The corrosion resistance of bipolar plate in cathode environment is worth to pay much attention because the

corrosion level of bipolar plate in cathode environment is more severe than that in anode. Potentiostatic curves of chromized SS 316L at cathode condition are shown in Fig. 5(b). The current density of sample A becomes stabilized quickly at the beginning and then maintains at a low level (about 6.5E−6 A cm^{-2}), while that of sample B is not as stable as that of sample A, it takes more time to obtain steady state. The current density of sample B is around 3.2E−5 A cm^{-2}, which is higher than that of sample A.

Results of potentiostatic tests of bare SS 316L in simulated PEMFC working conditions are in our early paper [24]. The current densities of bare SS 316L in anode and cathode condition are much higher than those of chromized SS 316L. The low current densities of chromized SS 316L indicate that chromizing treatments (both lower temperature chromizing treatment and conventional chromizing treatment) can enhance the corrosion resistance of SS 316L. In addition, the chromized SS 316L by lower temperature chromizing treatment exhibits better anticorrosion properties than that by conventional chromizing treatment. It could be due to the thicker chromized layer. Therefore, these results provide a convincing evidence to verify the benefit effect of chromium compounds produced by lower temperature chromizing treatment on protecting SS 316L against corrosion in a simulated PEMFC working environment.

3.3. ICR

ICR value of bipolar plate is one of the important parameters for PEMFC. Because decreasing ICR leads to the inner resistance of fuel cell to be decreased, and the output of fuel cell increased.

Fig. 6 indicates ICR value of bare SS 316L and chromized SS 316L by different chromizing processes as a function of compaction force. The decrease of ICR with increasing compaction force is due to the increasing of real contact area at high-compaction force. ICR value of chromized SS 316L is obvious lower than that of bare SS 316L. The ICR value is 13–25 mΩ cm^2 for chromized SS 316L and 45–55 mΩ cm^2 for bare SS 316L at a compaction force of 100–200 N cm^{-2}. Furthermore, ICR value of sample A is a little lower than that of sample B. Refer to previous studies [10,25,26], composition and roughness of the coating are the main factors to affect ICR. Chromized SS 316L shows lower ICR value than that of bare SS 316L, because the chromium carbide generated via pack chromization has better conductivity than that of chromium oxide. In addition, results of XRD and EDS represent that chromium nitride (Cr_2N) is also found in chromized coatings, which contribute to high conductivity of the coatings as well. Sample A exhibits better con-
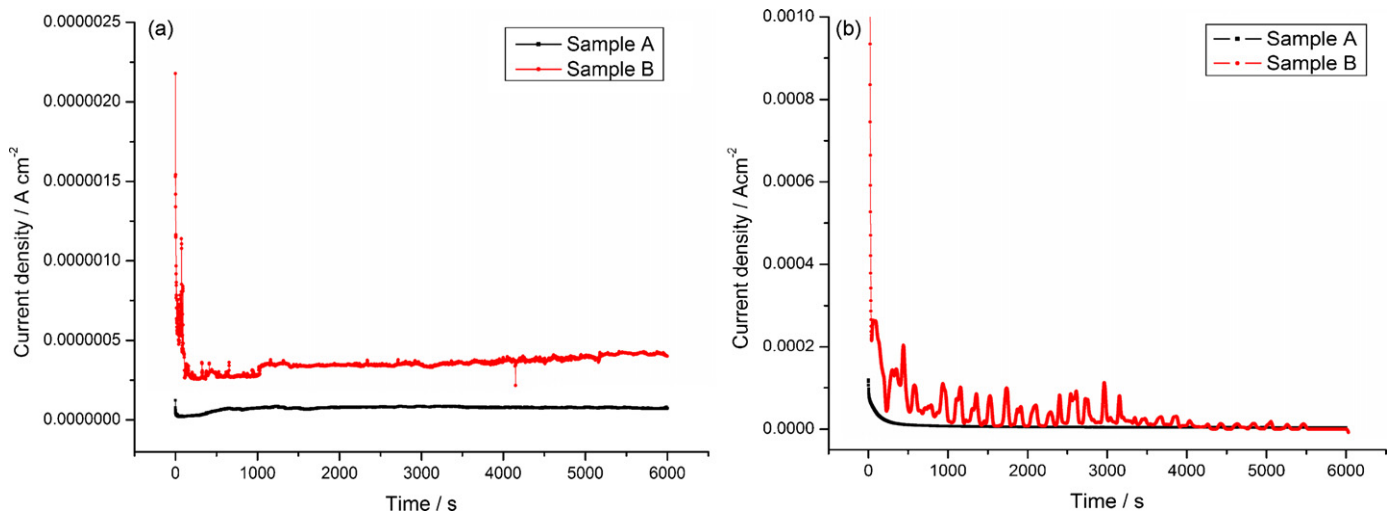

Fig. 5. Potentiostatic curves obtained from samples A and B: (a) at −0.1 V (versus SCE) purged with hydrogen gas and (b) at 0.6 V (versus SCE) purged with air at 70 °C.
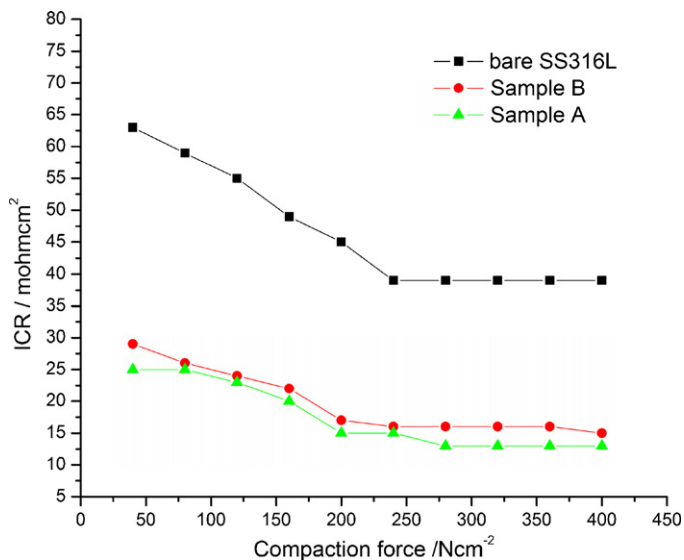
Fig. 6. ICR value of bare SS 316L, samples A and B as function of compaction force.

ductivity than that of sample B attributes to a higher content of chromium nitride. On the other hand, the difference in ICR values of samples A and B could be due to different roughness of surface. There is a specific or a range of roughness values, which can result in optimal lower contact resistance between bipolar plate and carbon paper. The roughness of sample A must be in the optimal range of an optimal effect.

4. Conclusions

SS 316L with Cr-enriched coating, prepared by lower temperature chromizing treatment, was tested and evaluated to act as an alternative material as bipolar plate for PEMFC. Potentiodynamic polarization results show that the chromized SS 316L exhibits the lowest passive current density about $3E-7\,A\,cm^{-2}$ that is about four orders of magnitude lower than that of bare SS 316L. In potentiostatic tests, the chromized SS 316L exhibits the stable corrosion current density, $7.5E-8\,A\,cm^{-2}$ at simulated anode condition and $6.5E-6\,A\,cm^{-2}$ at simulated cathode condition. Furthermore, the chromized SS 316L possess a much lower ICR value than that of bare SS 316L. The ICR value of bare SS 316L being $45\,m\Omega\,cm^2$ versus $13\,m\Omega\,cm^2$ for the chromized SS 316L under about $200\,N\,cm^{-2}$ compaction forces. Hence, the performance of the chromized SS 316L is comparable to that of graphite or noble metals for the application of bipolar plate for PEMFC. In this sense, the lower temperature chromizing treatment is considered to be the effective surface treatment to obtain high performance bipolar plate for PEMFC.

References

[1] B.L. Yi, Fuel Cell-theory Technology Application, 1st ed., Beijing, Chemical Industry Press, 2003, pp. 160–161.
[2] D.R. Hodgson, B. May, P.L. Adcock, D.P. Davies, J. Power Sources 96 (2001) 233–235.
[3] H. Tsuchiya, O. Kobayashi, Int. J. Hydrogen Energy 29 (2004) 985–990.
[4] B.D. Cunninghan, J. Huang, D.G. Baird, Int. Mater. Rev. 52 (2007) 1–13.
[5] H. Tawfik, Y. Hwang, D. Mahajan, J. Power Sources 163 (2007) 755–767.
[6] H. Wang, M.A. Sweikart, J.A. Turner, J. Power Sources 115 (2003) 243–251.
[7] K.H. Cho, W.G. Lee, S.B. Lee, H. Jang, J. Power Sources 180 (2008) 597–601.
[8] S.J. Lee, C.H. Huang, Y.P. Chen, J. Mater. Process. Technol. 140 (2003) 688–693.
[9] D.G. Nam, H.C. Lee, J. Power Sources 170 (2007) 268–274.
[10] S.B. Lee, K.H. Cho, W.G. Lee, H. Jang, J. Power Sources 187 (2009) 318–323.
[11] D.M. Miller, S.C. Kung, S.D. Scarberry, R.A. Rapp, Oxid. Met. 29 (1988) 239–254.
[12] F.D. Geib, R.A. Rapp, Oxid. Met. 40 (1993) 213–228.
[13] P.J. Ennis, A. Zielinska-Lipiec, O. Wachter, A. Czyrska-Filemonowicz, Acta Mater. 45 (1997) 4901.
[14] Z.D. Xiang, P.K. Datta, Surf. Coat. Technol. 184 (2004) 108.
[15] Z.B. Wang, J. Lu, K. Lu, Surf. Coat. Technol. 201 (2006) 2796–2801.
[16] Z.B. Wang, N.R. Tao, W.P. Tong, J. Lu, K. Lu, Acta Mater. 51 (2003) 4319.
[17] W.P. Tong, N.R. Tao, Z.B. Wang, J. Lu, K. Lu, Science 299 (2003) 686.
[18] Z.B. Wang, J. Lu, K. Lu, Acta Mater. 53 (2005) 2081–2089.
[19] Y. Wang, D.O. Northwood, J. Power Sources 163 (2006) 500–508.
[20] G. Hoogers, Fuel Cell Technology Handbook, CRC Press LLC, 2003, pp. 1–4.
[21] P.L. Hentall, J.B. Lakeman, G.O. Mepsted, P.L. Adcock, J.M. Moore, J. Power Sources 80 (1999) 235.
[22] L. Zancheva, M. Hillert, N. Lange, S. Seetharaman, L.-I. Staffansson, Metall. Trans. A 9 (1978) 909.
[23] R.E.E. Pulkkinen, J. Mater. Sci. Lett. 1 (1982) 421.
[24] H. Yu, L. Yang, L. Zhu, et al., J. Power Sources 191 (2009) 495–500.
[25] B. Avasarala, P. Haldar, J. Power Sources 188 (2009) 225.
[26] H. Wang, M.P. Brady, G. Teeter, J.A. Turner, J. Power Sources 138 (2004) 86–93.